Carbon Resources Conversion 7 (2024) 100183

Contents lists available at ScienceDirect

Carbon Resources Conversion

journal homepage: www.keaipublishing.com/en/journals/carbon-resources-conversion

Original Article

Co-production of hydrochar and bioactive compounds from *Ulva lactuca* via a hydrothermal process

Edy Hartulistiyoso [a,b], Obie Farobie [a,b,*], Latifa A Anis [b], Novi Syaftika [c], Asep Bayu [d], Apip Amrullah [e], Navid R. Moheimani [f], Surachai Karnjanakom [g], Yukihiko Matsumura [h]

[a] Department of Mechanical and Biosystem Engineering, IPB University, Bogor, West Java 16002, Indonesia
[b] Surfactant and Bioenergy Research Center (SBRC), IPB University, Bogor, West Java 16144, Indonesia
[c] Research Centre for Industrial Process and Manufacturing Technology, National Research and Innovation Agency (BRIN), Tangerang, Selatan, Indonesia
[d] Research Center for Vaccine and Drugs, National Research and Innovation Agency (BRIN), Bogor, West Java 16911, Indonesia
[e] Department of Mechanical Engineering, Lambung Mangkurat University, Banjarmasin, South Kalimantan, Indonesia
[f] Algae R&D Centre, Harry Butler Institute, Murdoch University, Murdoch, WA 6150, Australia
[g] Department of Chemistry, Rangsit University, Pathumthani 12000, Thailand
[h] Graduate School of Advanced Science and Engineering, Hiroshima University, 1-4-1 Kagamiyama, Higashi-Hiroshima 739-8527, Japan

ARTICLE INFO

Keywords:
Algae
Bioactive compound
Hydrochar
Hydrothermal
Seaweed

ABSTRACT

This study investigates the simultaneous production of hydrochar and bioactive compounds from *Ulva lactuca* via a hydrothermal process. The experiment was carried out using a batch reaction vessel at different reaction temperatures of 180–220 °C and various holding times of 30–90 min. As expected, both temperature and time vigorously influenced hydrochar and bioactive compound production. The maximum hydrochar yield was at 32.4 wt%. The higher heating value (HHV) of hydrochar was observed in the range of 17.68–21.07 MJ kg^{-1}, near the energy content of low-rank coals. The hydrochars exhibited contact angles higher than 90° (i.e., 94-108°) for a longer time, confirming their hydrophobic surfaces. The scanning electron microscope analysis (SEM) showed that the hydrothermal process enables cracks in the spherical shape of raw *U. lactuca* into small and porous particles. Besides producing hydrochar, the hydrothermal process of *U. lactuca* also gives promising antioxidants and phenolics as bioactive compounds. The highest total phenolic content and antioxidant activity could be achieved in hydrolysate at 200 °C and 30 min with the value of 1.20 ± 0.12 mg/g and 71.6 ± 1.3%, respectively.

1. Introduction

The sole reliance on fossil energy causes many environmental and economic problems. The current uncertain global political situation has also resulted in an unprecedented energy crisis [1]. Therefore, the transition to renewable energy, including biomass, to replace fossil fuels is strongly encouraged in various parts of the world. Moreover, renewable energy has been seen as one of the essential efforts to achieve Net Zero Emissions before or by 2050 that are targeted by many countries [2]. This is because biomass is considered carbon neutral, unlike fossil fuel, meaning that its burning will release carbon dioxide that is part of the biogenic carbon cycle.

The use of lignocellulosic biomass still faces pressures on land and fresh water-use competition, as well as the need for fertilizers [3,4]. As an alternative, macroalgae are an attractive option over terrestrial biomass since they are aquatic species that can grow in the ocean, have a high growth rate, do not require arable land, and contain high organic compounds [5].

As one of the countries with the longest coastline and largest ocean area worldwide, Indonesia has extraordinary marine organism biodiversity [6], including macroalgae, commonly known as seaweed. Seaweed has been used for centuries, mainly for food and medicines. In the modern era, Indonesia has been producing seaweed and has become the 2nd largest producer after China, with production accounting for 9.9 million tons in 2019 [7]. Nevertheless, the commercially utilized species are mostly *Gracilaria* sp., *Gelidium* sp., and *Eucheuma* sp., while other species remain less utilized. Moreover, Indonesian seaweed export is 80% in the form of raw materials with low added value, while processed products with higher economic benefits, such as food and pharmaceutical industry, are still in small share [8]. Realizing the great potential,

* Corresponding author at: Department of Mechanical and Biosystem Engineering, IPB University, Bogor, West Java 16002, Indonesia.
E-mail address: obiefarobie@apps.ipb.ac.id (O. Farobie).

https://doi.org/10.1016/j.crcon.2023.05.002
Received 13 January 2023; Received in revised form 20 April 2023; Accepted 11 May 2023
Available online 16 May 2023

Indonesia is encouraged to increase the utilization of seaweed and its added value by diversifying their product for food, feed, fertilizer, pharmaceutical, and cosmetics [9].

Meanwhile, Indonesia is working on achieving its Net Zero Emission (NZE) by 2060. One of the efforts is elevating the percentage of renewable energy from biomass in the national energy mix [10]. Intriguingly, with its organic content, macroalgae can be converted to solid fuel for energy sources, but this application path seems to be overlooked. Some studies showed that macroalgae could be the source generating hydrochar, using the hydrothermal process [11–13]. The hydrothermal technique uses hot compressed water, generally at 150–250 °C and elevated pressure, allowing a sequence of reactions to take place, including biomass decomposition and depolymerization, producing hydrochar with high content of carbon (up to 73%) and energy (15–30 MJ/kg) [14–16].

A study by Brown et al. in 2020 showed that the energy content of hydrochar from macroalgae *Saccharina latissima* and *Fucus serratus* increased by 47% and 172%, respectively, with the progress of the hydrothermal process [12]. A different study investigated activated hydrochar from *Euchema cottonii* exhibiting the formation of allotropes of carbon consisting of carbon microfibers and graphene [13]. Such porosity and functionality allow hydrochar to be used for various applications such as soil amendment, catalyst, adsorbent, and solid-combustion fuel [12]. Moreover, the energy densification ratio of hydrochar from macroalgae *Gelidium* sp. was observed by Patel et al. in 2021, ranging from 1.13 to 1.55, and can be categorized as a highly energy-dense product [11]. The solid fuel from macroalgae is expected to be applied so that the share of renewable energy to achieve the NZE target can be realized.

Macroalgae have a unique chemical composition, including bioactive materials such as sugars, phenolic compounds, and antioxidants [8,17]. These chemicals can be obtained in the liquid fraction along with the production of hydrochar using a hydrothermal process. This strategy is an example of a biorefinery framework to generate multiproduct that will increase the feasibility. However, the discussion on simultaneous hydrochar and high-value chemical production is still rare in the literature. *U. lactuca* is selected as a feedstock since it is abundantly available. Having said that, the bloom of *U. lactuca* can cause a significant problem in the marine biota due to the eutrophication problem. Hence, this study elaborated on using macroalgae *U. lactuca* to simultaneously obtain hydrochar and bioactive compounds, namely phenolic compounds and antioxidants.

2. Materials and methods

2.1. Characterization of U. Lactuca

The sample of *U. lactuca* was obtained from East Lombok beach, Nusa Tenggara Barat, Indonesia. The preparation of feedstock has been reported in our previous work [18]. In brief, the fresh *U. lactuca* was first cleaned with tap water to remove the sand and impurities. Subsequently, the wet *U. lactuca* biomass was dried under sunlight for around 6 h. The dried sample was then ground using a coffee bean grinder. Next, the sample was sieved to achieve a uniform particle size of 0.25 mm and stored in sacks for further analysis. Thermogravimetry analyses were carried out using a TGA 4000 thermogravimetric analyzer (Perkin Elmer, United States of America). This instrument was used to conduct proximate analysis under ASTM E1131-08. The ash content of *U. lactuca* was measured using the standard method of ASTM D1102. Our earlier works have informed the detailed proximate analysis [18,19].

Meanwhile, CHN628 (Leco, United States) was used to carry out the ultimate analysis of *U. lactuca* so that the carbon (C), hydrogen (H), and nitrogen (N) content could be measured. Moreover, CHN632 (Leco, United States) was used for sulfur (S) analysis. Finally, the remaining mass balance was expressed as oxygen (O) content. Moreover, a Parr 6200 bomb calorimeter (Isoperibol) was used to measure the HHV following the method of ASTM D 5865–04.

2.2. Hydrothermal process of U. Lactuca

A high-pressure reaction vessel (Berghof, Instruments GmbH, Germany) was used for the hydrothermal process of the *U. lactuca*. Fig. 1 shows a schematic diagram of a batch reactor. The feature of this reactor can be found in our previous work [19]. This reactor is available for use at elevated pressure and temperature (maximum pressure and temperature of 20 MPa and 300 °C, respectively).

The dried macroalgae with a particle size of 0.25 mm were mixed with distilled water so that the concentration obtained was 5 wt%. The mixture was placed into the reactor, and then the reaction vessel was closed securely with a top cover and purged with purified nitrogen gas to eliminate the air. The hydrothermal experiment was carried out at 180, 200, and 220 °C for 30, 60, and 90 min of holding times at a pressure of approximately 8 MPa. Once the hydrothermal process was completed, the reactor heater was switched off. Afterward, an ice water chamber cooled down the reaction vessel immediately. Next, the sample inside the reactor was moved to a beaker glass. Then, the solid product (hydrochar) was removed from the aqueous product (hydrolysate) by filtration using a vacuum pump. Subsequently, the solid product was oven-dried for 24 h at 105 °C. Please note that triple-replicate experiments were conducted. The yields of the product were calculated using the following equations [11]:

$$\text{Liquid(hydrolysate)yield } (\%) = \frac{W_{liquidafterfiltration}}{W_{initialfeedstock}} \times 100 \quad (1)$$

$$\text{Solidyield } (\%) = \frac{W_{solidproductafterfiltration}}{W_{initialfeedstock}} \times 100 \quad (2)$$

$$\text{Gasyield } (\%) = 100 - (solidyield\% + liquidyield\%) \quad (3)$$

Meanwhile, equation (4) was employed to determine the energy densification ratio [11]:

$$\text{Energydensificationratio } (-) = \frac{HHV_{hydrochar}}{HHV_{initialfeedstock}} \quad (4)$$

2.3. Characterization of hydrochar

The hydrochar obtained from the hydrothermal process was examined concerning ultimate analyses, higher heating values (HHVs), surface morphology, functional group, and contact angle. As mentioned previously, the protocol to measure the elemental composition and the HHV of hydrochar product is the same as the one applied for *U. lactuca*.

A Fourier Transform Infrared (FTIR) spectrometer (Perkin Elmer, United States) was applied to identify the functional groups of untreated *U. lactuca* and its derived hydrochar. As a result, FTIR spectra were obtained in the wavenumber ranging from 400 to 4000 cm^{-1}. Moreover, an SU 3500 Scanning Electron Microscope (Hitachi, Japan) was employed to examine the imaging characterization of feedstock *U. lactuca* and its corresponding product of hydrochars. Meanwhile, surface contact angle analysis was performed using a JC2000D1 contact angle tester (Shanghai Zhongshan Digital Technology Equipment Co. Ltd., China). This contact angle instrument was equipped with a high-resolution CCD camera.

2.4. Characterization of hydrolysate

The analysis of total phenolic content, antioxidant activity, and UV-absorbance was employed to characterize the hydrolysate, the aqueous phase of the hydrothermal process. To calculate the total phenolic content of *U. lactuca* hydrolysate, we used the Folin-Ciocalteau method. The detailed protocol to determine total phenolic content can be found in the previous works [19–21]. In summary, the absorbance of the

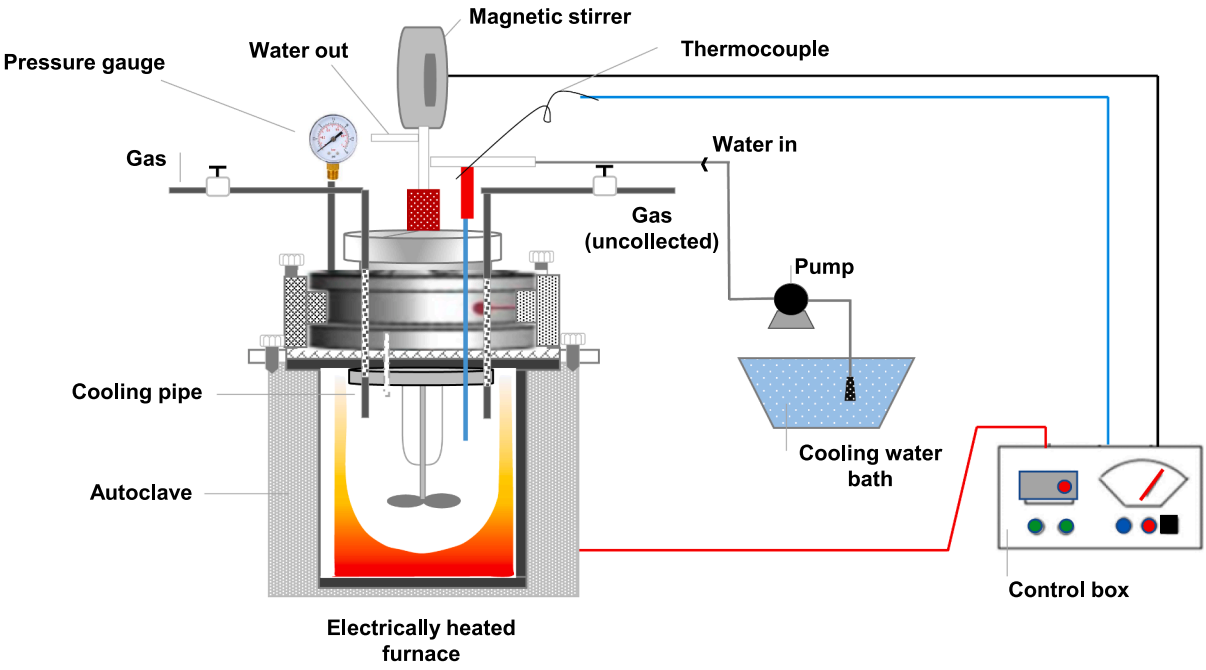

Fig. 1. A schematical diagram of the experimental apparatus.

sample mixture and the Folin-Ciocalteau's phenol reagent was determined using a UV–Vis Spectrophotometer at 750 nm. The standard curve of gallic acid solution calculates the total phenolic content (TPC). Moreover, the value of TPC was determined as a mass of gallic acid equivalent (GAE) per mass of samples (mg GAE/g).

The antioxidant activity of *U. lactuca* hydrolysate was determined using a 2,2-diphenyl-1-picrylhydrazyl (DPPH) method [19,22]. The mixture of the sample and DPPH reagent was determined using a UV–Vis spectrophotometer at 515 nm. The scavenging effect (%) was determined using equation (5):

$$\text{Scavenging effect}\,(\%) = \frac{A_c - A_s}{A_c} \times 100 \tag{5}$$

Where, A_s and A_c represent the sample and control reaction absorbance, respectively.

Meanwhile, a U-2900 UV–Vis spectrophotometer (Hitachi, Japan) was used to determine the UV-absorbance of hydrolysate. Three repeated measures were performed for all analyses.

3. Results and discussion

3.1. Product yield

Temperature, as well as time, are the most significant parameters influencing liquid, solid, and gas product distribution. As Stemann et al. (2013) reported, temperature enables the decomposition of macromolecular biomass structures [23]. The change in product distribution of the hydrothermal process of *U. lactuca* with temperature and holding time is shown in Fig. 2. Increasing temperature and prolonging reaction time leads to a decrease in hydrochar yield (Fig. 2). Hydrochar yields decreased from 32.43 wt% to 28.22 wt% once the temperature was raised from 180 to 200 °C for 30 min reaction time. The hydrochar yield gradually dropped to approximately 24.15 wt% as the temperature rose further to 220 °C. This can be explained because the increased temperature could enhance the carbonization and more substantial primary decomposition of macromolecules generating liquid and gas products [24]. Roman et al. (2018) reported that various decomposition reactions occur on the intermediates generated during the hydrothermal process of biomass, such as dehydration, deoxygenation, and aromatization, resulting in the production of liquid and gas products, and causing a decrease in solid product [25].

The product yield changes during the hydrothermal are in accordance with the earlier works [11,12]. In addition, hot compressed water in the hydrothermal process could suppress the mass transfer limitation, causing lower activation energy [26,27]. Consequently, the hydrothermal process enables better penetration into porous biomass, making it easy to decompose into liquid and gas products, resulting in biomass deterioration [28]. Partridge et al. (2020) also postulated that during the hydrothermal process, the hemicellulose initially decomposed at the temperature range of 180–200 °C. The hydrolysis of cellulose, representing the significant loss of hydrochar occurred as the temperature is further increased beyond 200 °C [29].

Unlike the solid trend, the extended reaction time from 10 to 20 min resulted in an enhancement in liquid product from 62.40 wt% to 64.26 wt% at 180 °C. However, the liquid yield slightly dropped to about 63.49 wt% with an extended time of 30 min. Increasing liquid yield with time from 10 to 20 min might be because the main decomposition reactions, primarily due to thermal cracking and dehydration, were enhanced. In the meantime, extending the reaction time to 30 min might cause further product decomposition, improving gaseous products instead of pertaining to the liquid phase. Nevertheless, at higher temperatures, 200 and 220 °C, the liquid yield gradually decreased once the holding time was extended. This can be explained because higher temperatures and longer reaction times led to complete carbonization, causing a lower liquid yield [30,31]. Apart from that, under more severe conditions at elevated temperatures and times, the simple compounds in the liquid phase having low molecular weight were also thermally cracked to generate non-condensable gas [32–34]. The trend of gas yield proved this, which increased with temperature and time.

3.2. Higher heating value and energy densification ratio of hydrochar

The change in HHV and energy densification ratio with temperature and holding time during the hydrothermal process is presented in Table 1. The energy densification ratios of hydrochar obtained at the operating temperatures of 180–220 °C and times of 30–90 min were between 1.47 and 1.75. Since the energy densification ratio of hydrochar is above 1.00, it confirms that hydrothermal processing enabled the

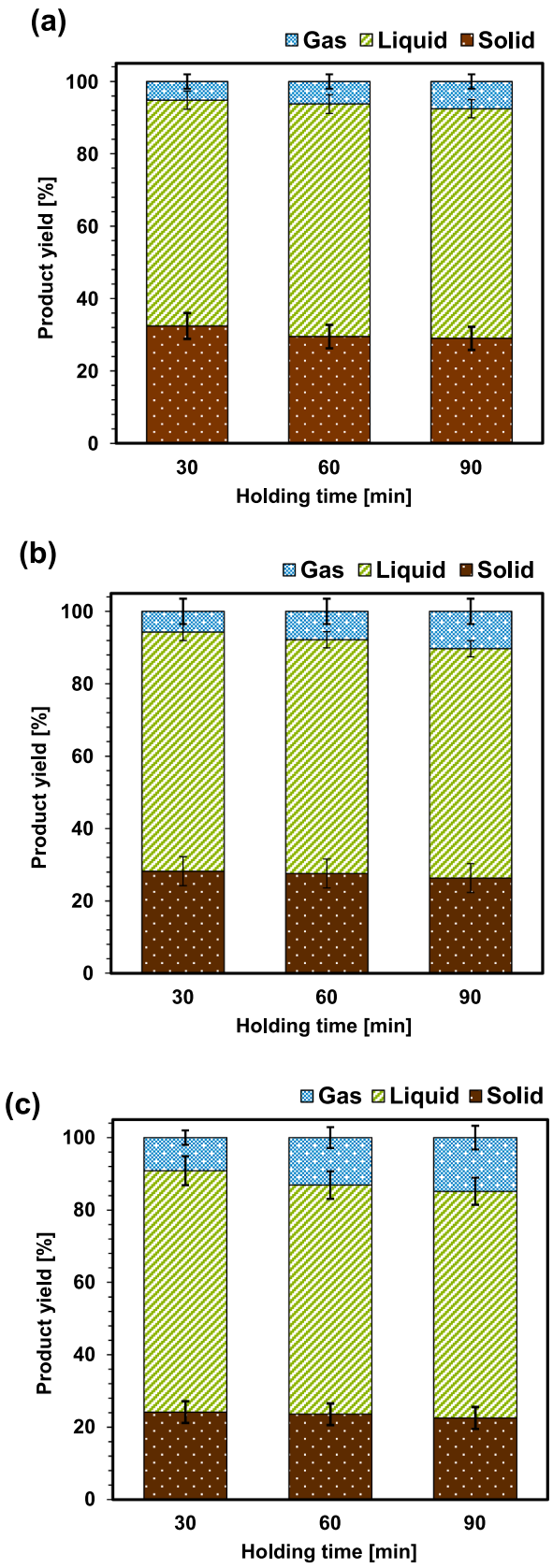

Fig. 2. Product distribution of hydrothermal process of *U. lactuca* at (a) 180 °C, (b) 200 °C, and (c) 220 °C.

Table 1
The higher heating value (HHV) and energy analysis of hydrochar derived from *U. lactuca*.

Parameters		HHV (MJ/kg)	Energy densification ratio [-]
Temperature [°C]	Holding time [min]		
180	30	17.68 ± 0.19	1.47
180	60	17.95 ± 0.21	1.49
180	90	18.06 ± 0.26	1.50
200	30	18.11 ± 0.31	1.50
200	60	18.76 ± 0.38	1.56
200	90	19.06 ± 0.14	1.58
220	30	19.60 ± 0.21	1.63
220	60	19.93 ± 0.18	1.66
220	90	21.07 ± 0.14	1.75

production of energy-dense hydrochar.

Moreover, increasing temperature and extending holding time led to the rise of the HHV of the hydrochar. As the temperature was elevated from 180 to 220 °C, the HHV of hydrochar raised by over 10.86%, 11.03%, and 16.67% at the reaction time of 30, 60, and 90 min, respectively. Therefore, it might be associated with decarboxylation and dehydration reaction, which could enhance the carbon content in hydrochar, causing an increase in HHV [11,35–37]. As a result, the HHV of hydrochar was between 17.68 and 21.07 MJ kg^{-1}, which is comparable with the energy content of the low-rank coals. The HHVs of low-rank coals are in the range of 12–25 MJ kg^{-1} with an average value of 15 MJ kg^{-1}, as Luo and Tao (2017) reported [38].

3.3. Elemental composition of hydrochar

The elemental composition of hydrochar derived from the hydrothermal process of *U. lactuca* at various operating conditions is presented in Table 2. In general, increasing temperature and extending time enhanced the carbon content of *U. lactuca*. The carbon content rose from 39.10% in untreated U. lactuca to 48.20% in hydrochar after hydrothermal. This might be due to dehydration and aromatization at elevated temperatures [24,33,39]. It is noteworthy to mention that the enhancement of carbon content in hydrochar is helpful for carbon dioxide sequestration. Since its carbon component is generally stable, increasing carbon content results in more carbon fixed in the soil as char, enhancing carbon dioxide sequestration. A relatively stable form of carbon has the potential to serve as an effective long-term carbon store and have a significant impact on the reduction of greenhouse gas emissions. It can also be linked because increasing carbon content in hydrochar as a porous material can enhance its capacity to adsorb and retain carbon dioxide, thus improving its effectiveness for carbon dioxide sequestration [40].

In contrast, increasing temperature and extending time resulted in a slight decrease in oxygen contents from 31.06% in the raw *U. lactuca* to 28.24% in the hydrochar at the operating conditions observed in this study. It should be attributed to the decarboxylation and dehydration reactions [41]. Similarly to the oxygen content, the hydrothermal process could reduce nitrogen from 4.46% in the raw *U. lactuca* to 3.05% in the hydrochar. The decreasing nitrogen content during the hydrothermal process could be related to the degradation of protein-containing nitrogen released from macroalgae into the liquid phase [42].

Furthermore, the effect of hydrothermal temperature and time on ash content was investigated. It was found that temperature and time

Table 2
Elemental composition of *U. lactuca* and its corresponding hydrochar.

Sample	Ultimate analysis (wt%)					Ash (wt%)
	% C	% H	% N	% S	% O	
Raw feedstock (*U. lactuca*)	39.10 ± 0.30	6.2 ± 0.03	4.46 ± 0.02	7.28 ± 0.03	31.06 ± 0.45	11.90
Hydrochar (180 °C, 30 min)	43.98 ± 0.16	5.12 ± 0.06	4.04 ± 0.03	6.77 ± 0.07	28.68 ± 0.29	11.41
Hydrochar (180 °C, 60 min)	44.39 ± 0.21	5.02 ± 0.10	3.94 ± 0.07	6.91 ± 0.04	28.48 ± 0.32	11.25
Hydrochar (180 °C, 90 min)	45.25 ± 0.14	4.91 ± 0.08	3.88 ± 0.02	7.15 ± 0.02	27.76 ± 0.24	11.04
Hydrochar (200 °C, 30 min)	45.87 ± 0.19	5.00 ± 0.11	3.53 ± 0.09	7.08 ± 0.06	28.05 ± 0.31	10.47
Hydrochar (200 °C, 60 min)	46.08 ± 0.24	4.53 ± 0.04	3.49 ± 0.04	7.51 ± 0.11	28.17 ± 0.28	10.22
Hydrochar (200 °C, 90 min)	47.29 ± 0.14	4.11 ± 0.03	3.39 ± 0.06	6.93 ± 0.07	28.33 ± 0.36	9.94
Hydrochar (220 °C, 30 min)	47.58 ± 0.19	4.01 ± 0.05	3.30 ± 0.08	8.24 ± 0.09	27.44 ± 0.35	9.43
Hydrochar (220 °C, 60 min)	47.68 ± 0.17	3.93 ± 0.08	3.13 ± 0.06	8.58 ± 0.03	27.44 ± 0.26	9.24
Hydrochar (220 °C, 90 min)	48.20 ± 0.24	3.40 ± 0.11	3.05 ± 0.05	7.94 ± 0.12	28.24 ± 0.19	9.17

significantly affected the ash content ($P < 0.05$). It is important to note that the ash content was reduced with hydrothermal temperature and duration increment. The decrease in ash content with increasing hydrothermal process temperature and time can be attributed to removing minerals from the feedstock during the hydrothermal process. Since the hydrothermal process uses water as a medium, some minerals in the feedstock, such as potassium, calcium, etc., can be dissolved in the water during the hydrothermal process. As a result, they are removed from the solid material. In addition, as the temperature and time of the hydrothermal process increase, the solubility of these minerals in the water also increases, leading to more significant removal of these minerals.

To compare the O/C and H/C atomic ratios between untreated feedstock and hydrochar, a van Krevelen diagram is presented in Fig. 3. As shown in the diagram, more severe conditions at elevated temperatures and times led to a drop in the O/C and H/C atomic ratios. The O/C and H/C atomic ratios of untreated feedstock were 0.59 and 1.90, respectively. In the meantime, the O/C and H/C atomic ratios of hydrochar were achieved at about 0.44 and 0.85, respectively, at 220 °C and 90 min. It should be due to decarboxylation and dehydration reactions via breaking the carbon–oxygen bond of ester and ether in biomass [43,44].

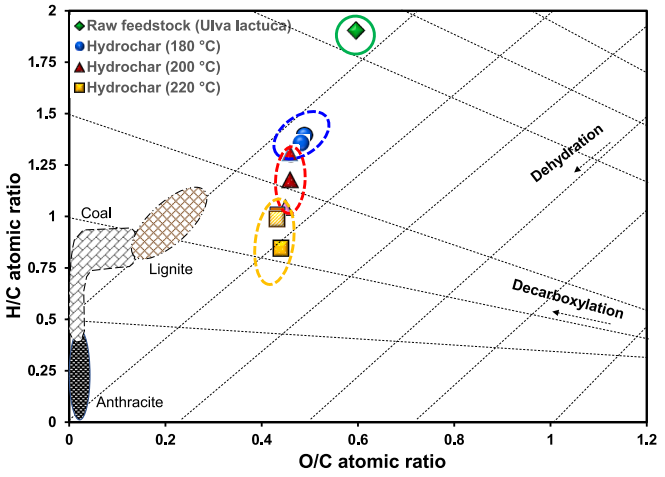

Fig. 3. van Krevelen diagram of *U. lactuca* and its corresponding hydrochar.

3.4. SEM images and functional groups of hydrochar

The morphological change during the hydrothermal process of raw *U. lactuca* was observed by SEM. Images of untreated *U. lactuca* and its derived hydrochar are depicted in Fig. 4. It is clearly shown that the hydrothermal process could significantly alter the surface morphology of *U. lactuca*. The hydrothermal process enables cracks in the spherical shape of raw *U. lactuca* into small and porous particles with rough surfaces. In addition, the formation of mesoporous particles was also found in the hydrochar that evolved from several kinds of feedstocks [45–47]. The mesoporous particles in hydrochar are thought to be generated due to the deformation of the chemical bond in raw feedstock and the discharge of volatile compounds at elevated temperatures [48,49]. Furthermore, it is also postulated owing to the hydrothermal process of cellulose and other carbohydrate compounds [50,51].

The functional groups of raw *U. lactuca* and its derived hydrochar were also investigated by FTIR. Fig. 5 shows the FTIR spectra of untreated *U. lactuca* and its derived hydrochar. Both raw *U. lactuca* and its derived hydrochar had a wide peak at 3000–3300 cm^{-1}, assigned to the vibration of –OH stretching from the hydroxyl and carboxyl functional groups [46]. Nevertheless, this band weakened or even disappeared once the operating condition was elevated from 180 °C to 200 °C and 220 °C, confirming the dehydration at elevated temperatures. The aliphatic C–H medium bands stretching at 2852–2918 cm^{-1} were identified in hydrochar. The strong peak at 1628–1636 cm^{-1} was observed at raw feedstock and its hydrochar, attributed to the aromatic C═C ring stretching [52]. Moreover, the aromatic C–H group with the stretching vibrations was also observed, with evidence of strong peaks at 1027–1032 cm^{-1}. Interestingly, few peaks were observed around 400–700 cm^{-1} in hydrochar, but this is not the case for raw feedstock. These peaks correlate to the presence of polycyclic aromatic compounds in hydrochar [53].

3.5. Contact angle of hydrochar

The contact angle of hydrochar was observed to examine the hydrophobicity of biomass. The contact angle of raw *U. lactuca* and its corresponding hydrochar are depicted in Fig. 6. It should be noted that the contact angle above 90° correlated to a hydrophobic surface. Meanwhile, with the contact angle below 90°, the sample's surface is more hydrophilic. Once the contact angle is close to 0°, the surface is entirely hydrophilic, which tends to be hygroscopic property.

As observed in Fig. 6, for the case of raw *U. lactuca*, the initial contact angle is 64°. At around 4 s, the angle of *U. lactuca* becomes 0°, confirming its hydrophilicity. It could be attributed to the fact that raw *U. lactuca* contains hydroxyl groups (–OH) from carbohydrates soluble in water via hydrogen bonding interaction [54].

In contrast with the raw *U. lactuca*, the hydrochar exhibited contact angles higher than 90° for a longer time, indicating that hydrochar is more hydrophobic than hydrophilic. The higher the temperature of the hydrothermal process, the greater the contact angle. Hydrochar derived from *U. lactuca* has contact angles in the ranges of 94-108°. This finding reveals that the transformational property of macroalgae from hydrophilic to hydrophobic after hydrothermal can considerably enhance their stability, causing the improvement of CO_2 sequestration ability. It should be noted that the hydrophobicity of produced hydrochar can help enhance its stability and carbon sequestration since hydrophobicity can prevent hydorchar from absorbing water, reducing degradation through water exposure, and increasing its stability in the soil.

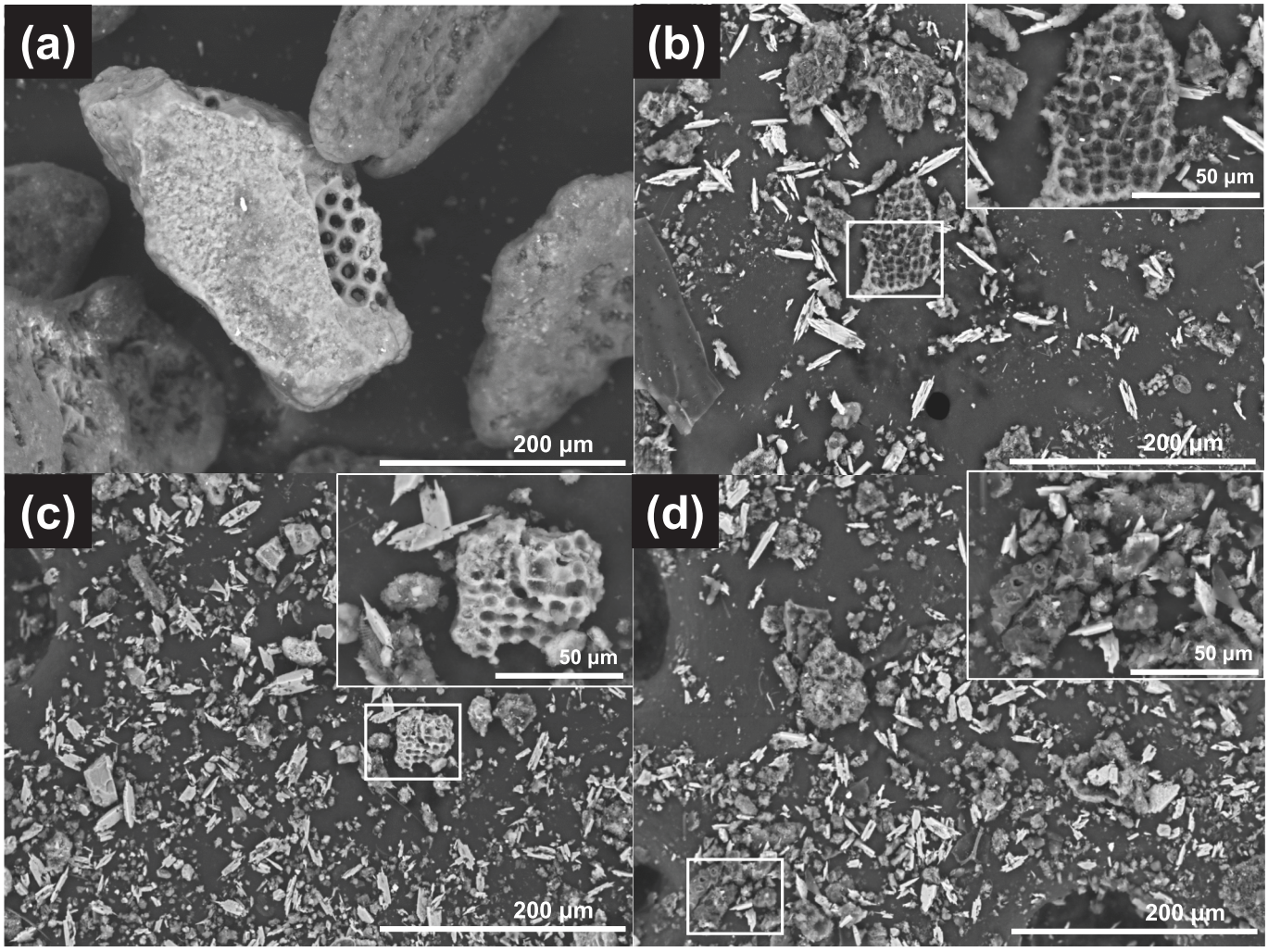

Fig. 4. SEM images of (a) raw *U. lactuca* and hydrochar at (b) 180 °C, (c) 200 °C, and (d) 220 °C.

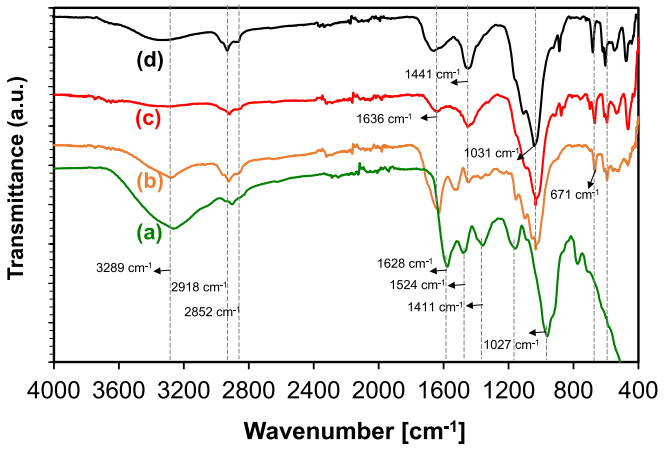

Fig. 5. FTIR spectra of (a) raw *U. lactuca* and hydrochar at (b) 180 °C, (c) 200 °C, and (d) 220 °C.

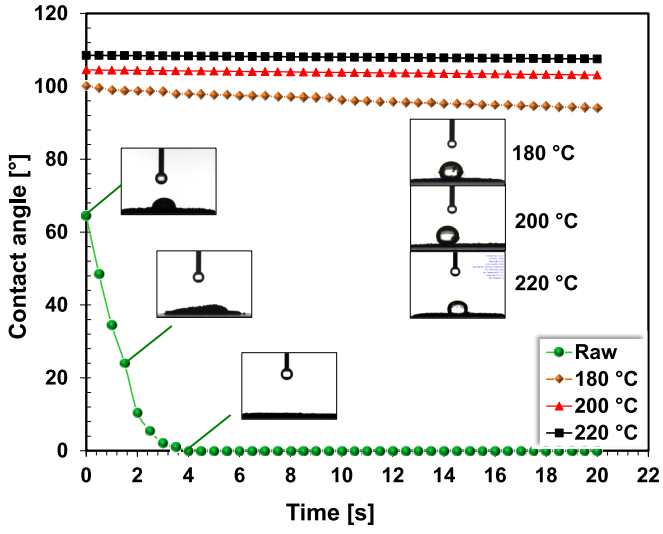

Fig. 6. Contact angle profile of raw *U. lactuca* and its corresponding hydrochar.

3.6. Phenolic content and antioxidant activities of hydrolysate

Fig. 7 shows the total phenolic content, the ability of DPPH-radical scavenging, and the UV-absorbance of U. lactuca hydrolysate at various temperatures. As depicted in Fig. 7 (a), increasing the operating condition from 180 °C to 200 °C at reaction times of 30 and 60 min increased the total phenolic content of U. lactuca hydrolysate. The total content of phenolic compounds was identified to be the highest (1.20 ± 0.11 mg/g) in U. lactuca hydrolysate at 200 °C and 30 min. It should be because increasing temperature from 180 °C to 200 °C resulted in more

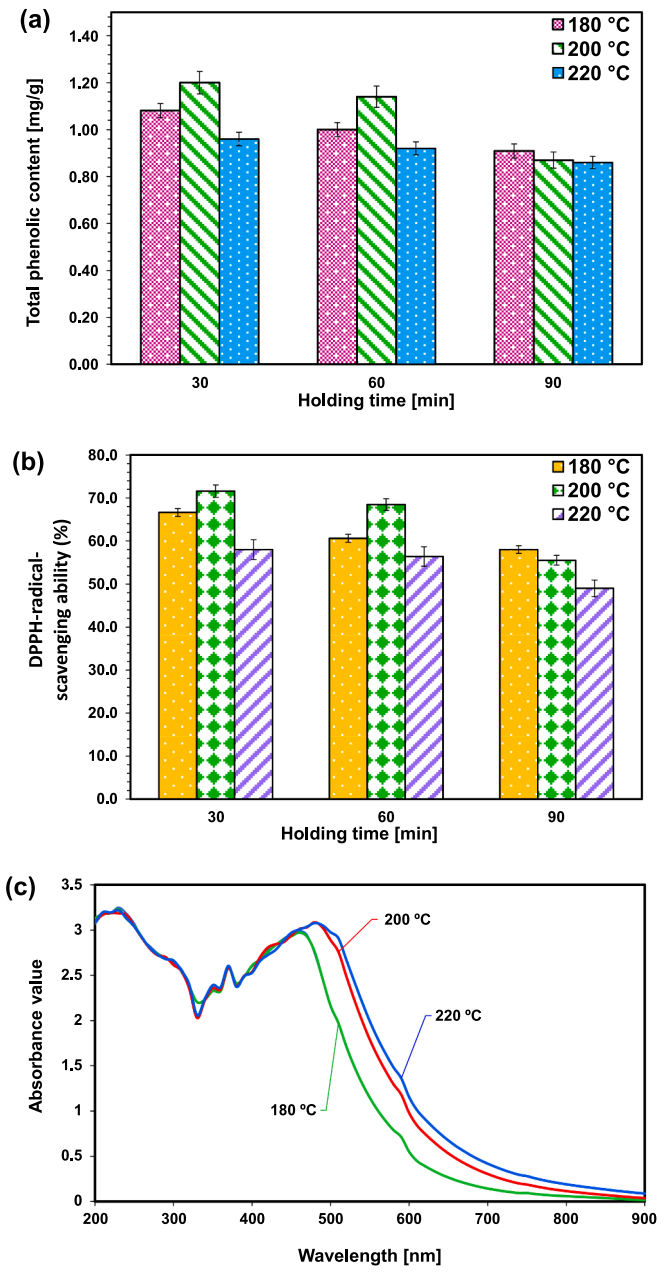

Fig. 7. (a) total phenolic content, (b) antioxidant activity, and (c) UV-absorbance spectra of *U. lactuca* hydrolysate.

nonpolar phenolic compounds being extracted owing to lowering the value of the water dielectric constant [55]. Nevertheless, at more severe temperatures higher than 200 °C and longer holding time at 90 min, the total phenolic constant declined due to the thermal decomposition of phenolic compounds under higher severity conditions.

The potential antioxidant activity of *U. lactuca* hydrolysate was determined using DPPH free radical scavenging assay. The DPPH-radical-scavenging ability of *U. lactuca* hydrolysate at various operating conditions is presented in Fig. 7 (b). As observed, the antioxidant activity increased considerably with temperature observed from 180 to 200 °C. It could be due to the more nutritional compounds, such as flavonoid and phenolic compounds, extracted at 200 °C. However, at a temperature beyond 200 °C, the antioxidant activity decreased due to nutritional compounds' decomposition. This work confirms that the hydrolysate of macroalgae *U. lactuca* can be a valuable material for bioactive compounds.

Fig. 7 (c) presents the UV absorption spectra of *U. lactuca* hydrolysate. The absorption band at 230 nm was observed, corresponding to the transition of n → π* orbital for —C═O (carbonyl) or —COOH (carboxyl) groups. Moreover, the sharp absorption band at 460 nm was assigned to the change of n → π* orbital for the —N═O (nitroso) groups [56]. The peak was shifted to the longer wavelength at 480 nm once the operating temperature was raised to 200 and 220 °C. It should be linked to the movement of auxochrome groups with the temperature.

4. Conclusion

Concurrent production of hydrochar and bioactive compounds from macroalgae *U. lactuca* via a hydrothermal method was successfully conducted. The maximum total phenolic content (1.20 ± 0.12 mg/g) and antioxidant activity (71.6 ± 1.3%) were obtained from *U. lactuca* hydrolysate at 200 °C and 30 min. At the same time, the yield of hydrochar (28.2 wt%) was also obtained. Based on the van Krevelen diagram, more severe conditions at elevated temperatures and times decreased the O/C and H/C atomic ratios. The energy densification ratios of hydrochar were reported between 1.47 and 1.75, indicating that hydrothermal processing enabled the production of energy-dense hydrochar. The hydrochar exhibits a calorific value of 17.68–21.07 MJ kg^{-1}, which is similar to the low-rank coals. Moreover, the hydrochar exhibited contact angles higher than 90° (i.e., 94-108°) for a longer time, confirming their hydrophobic surfaces. Overall, this work provides insights into hydrochar and bioactive compounds that could be obtained simultaneously from *U. lactuca* via a hydrothermal process.

CRediT authorship contribution statement

Edy Hartulistiyoso: Conceptualization, Methodology, Writing – original draft, Resources. **Obie Farobie:** Conceptualization, Funding acquisition, Writing – original draft, Data curation, Supervision, Project administration. **Latifa A Anis:** Methodology, Investigation, Data curation. **Novi Syaftika:** Investigation, Writing – review & editing, Resources. **Asep Bayu:** Investigation, Writing – review & editing, Resources. **Apip Amrullah:** Methodology, Formal analysis, Resources. **Navid R. Moheimani:** Conceptualization, Writing – review & editing. **Surachai Karnjanakom:** Conceptualization, Writing – review & editing. **Yukihiko Matsumura:** Supervision, Writing – review & editing.

Declaration of Competing Interest

The authors declare that they have no known competing financial interests or personal relationships that could have appeared to influence the work reported in this paper.

Acknowledgments

This project was supported financially by the Indonesian Endowment Fund for Education (LPDP) through "RISPRO KI" the International Research Collaboration (Grant No. RISPRO/KI/B1/KOM/12/11684 /1/2020).

References

[1] B. Steffen, A. Patt, A historical turning point? Early evidence on how the Russia-Ukraine war changes public support for clean energy policies, Energy Res. Soc. Sci. 91 (2022), 102758, https://doi.org/10.1016/j.erss.2022.102758.

[2] I. Ko, N. Dolšak, A. Prakash, Have renewable energy leaders announced aggressive emission reduction goals? Examining variations in the stringency of country-level net-zero emission pledges, PLOS Clim. 1 (2022) e0000094.

[3] O. Farobie, Y. Matsumura, N. Syaftika, A. Amrullah, E. Hartulistiyoso, A. Bayu, N. R. Moheimani, S. Karnjanakom, G. Saefurahman, Recent advancement on hydrogen production from macroalgae via supercritical water gasification, Bioresour. Technol. Reports. 16 (2021), 100844, https://doi.org/10.1016/j.biteb.2021.100844.

[4] J.M. Greene, J. Gulden, G. Wood, M. Huesemann, J.C. Quinn, Techno-economic analysis and global warming potential of a novel offshore macroalgae biorefinery, Algal Res. 51 (2020), https://doi.org/10.1016/j.algal.2020.102032.
[5] J.J. Milledge, B. Smith, P.W. Dyer, P. Harvey, Macroalgae-derived biofuel: A review of methods of energy extraction from seaweed biomass, Energies. 7 (2014) 7194–7222, https://doi.org/10.3390/en7117194.
[6] M. Hutomo, M.K. Moosa, Indonesian marine and coastal biodiversity: Present status, Indian J. Mar. Sci. 34 (2005) 88–97.
[7] O. Farobie, N. Syaftika, E. Hartulistiyoso, A. Amrullah, A. Bayu, N.R. Moheimani, Y. Matsumura, S. Karnjanakom, The Potential of Sustainable Biogas Production from Macroalgae in Indonesia, IOP Conf. Ser. Earth Environ. Sci. 1038 (2022), https://doi.org/10.1088/1755-1315/1038/1/012020.
[8] R. Pangestuti, M. Haq, P. Rahmadi, B.S. Chun, Nutritional value and biofunctionalities of two edible green seaweeds (Ulva lactuca and caulerpa racemosa) from indonesia by subcritical water hydrolysis, Mar. Drugs. 19 (2021) 578, https://doi.org/10.3390/md19100578.
[9] M.A. Rimmer, S. Larson, I. Lapong, A.H. Purnomo, P.R. Pong-masak, L. Swanepoel, N.A. Paul, Seaweed aquaculture in indonesia contributes to social and economic aspects of livelihoods and community wellbeing, Sustain. 13 (2021) 1–22, https://doi.org/10.3390/su131910946.
[10] O. Farobie, E. Hartulistiyoso, Palm Oil Biodiesel as a Renewable Energy Resource in Indonesia: Current Status and Challenges, Bioenergy Res. 15 (2022) 93–111, https://doi.org/10.1007/s12155-021-10344-7.
[11] N. Patel, B. Acharya, P. Basu, Hydrothermal carbonization (Htc) of seaweed (macroalgae) for producing hydrochar, Energies. 14 (2021) 1–16, https://doi.org/10.3390/en14071805.
[12] A.E. Brown, G.L. Finnerty, M.A. Camargo-Valero, A.B. Ross, Valorisation of macroalgae via the integration of hydrothermal carbonisation and anaerobic digestion, Bioresour. Technol. 312 (2020), 123539, https://doi.org/10.1016/j.biortech.2020.123539.
[13] T. Prakoso, R. Nurastuti, R. Hendriansyah, J. Rizkiana, G. Suantika, G. Guan, Hydrothermal Carbonization of Seaweed for Advanced Biochar Production, MATEC Web Conf. 156 (2018) 05012.
[14] R. Babu, G. Capannelli, M. Bernardini, M. Pagliero, A. Comite, Effect of varying hydrothermal temperature, time, and sludge pH on sludge solubilisation, Carbon Resour. Convers. 6 (2022) 142–149, https://doi.org/10.1016/j.crcon.2022.12.001.
[15] C.S. Liew, W. Kiatkittipong, J.W. Lim, M.K. Lam, Y.C. Ho, C.D. Ho, S.K. O. Ntwampe, M. Mohamad, A. Usman, Stabilization of heavy metals loaded sewage sludge: Reviewing conventional to state-of-the-art thermal treatments in achieving energy sustainability, Chemosphere. 277 (2021), 130310, https://doi.org/10.1016/j.chemosphere.2021.130310.
[16] C. Peng, G. Zhang, J. Han, X. Li, Hydrothermal conversion of lignin and black liquor for phenolics with the aids of alkali and hydrogen donor, Carbon Resour. Convers. 2 (2019) 141–150, https://doi.org/10.1016/j.crcon.2019.06.004.
[17] A. Bayu, T. Handayani, High-value chemicals from marine macroalgae: Opportunities and challenges for marine-based bioenergy development, IOP Conf. Ser. Earth Environ. Sci. 209 (2018), https://doi.org/10.1088/1755-1315/209/1/012046.
[18] O. Farobie, N. Syaftika, I. Masfuri, T.P. Rini, D.P.A. Lanank Es, A. Bayu, A. Amrullah, E. Hartulistiyoso, N.R. Moheimani, S. Karnjanakom, Y. Matsumura, Green algae to green fuels: Syngas and hydrochar production from Ulva lactuca via sub-critical water gasification, Algal Res. 67 (2022), 102834, https://doi.org/10.1016/j.algal.2022.102834.
[19] O. Farobie, L.A. Anis, W. Fatriasari, A. Karimah, P.R. Nurcahyani, D.Y. Rahman, A. L. Nafisyah, A. Amrullah, M. Aziz, Simultaneous production of nutritional compounds and hydrochar from Chlorella pyrenoidosa via hydrothermal process, Bioresour. Technol. Reports. 20 (2022), 101245, https://doi.org/10.1016/j.biteb.2022.101245.
[20] N. Saeed, M.R. Khan, M. Shabbir, Antioxidant activity, total phenolic and total flavonoid contents of whole plant extracts Torilis leptophylla L, BMC Complement. Altern. Med. 12 (2012) 221, https://doi.org/10.1186/1472-6882-12-221.
[21] H. Rawindran, J.W. Lim, V. Rao Pasupuleti, L. Wai Hong, I. Julian Dinshaw, L. C. Seng, N. Tasnim Binti Sahrin, R. Raksasat, F. Musa Ardo, Impact of Various Concentration of Phenol and p-Chlorophenol to the Microalgal Population in Wastewater, CJST 10 (02) (2022) 24–30.
[22] S.A. Baba, S.A. Malik, Determination of total phenolic and flavonoid content, antimicrobial and antioxidant activity of a root extract of Arisaema jacquemontii Blume, J. Taibah Univ. Sci. 9 (2015) 449–454, https://doi.org/10.1016/j.jtusci.2014.11.001.
[23] J. Stemann, A. Putschew, F. Ziegler, Hydrothermal carbonization: Process water characterization and effects of water recirculation, Bioresour. Technol. 143 (2013) 139–146, https://doi.org/10.1016/j.biortech.2013.05.098.
[24] C.G. Khoo, M.K. Lam, A.R. Mohamed, K.T. Lee, Hydrochar production from high-ash low-lipid microalgal biomass via hydrothermal carbonization: Effects of operational parameters and products characterization, Environ. Res. 188 (2020), 109828, https://doi.org/10.1016/j.envres.2020.109828.
[25] S. Román, J. Libra, N. Berge, E. Sabio, K. Ro, L. Li, B. Ledesma, A. Alvarez, S. Bae, Hydrothermal carbonization: Modeling, final properties design and applications: A review, Energies. 11 (2018) 1–28, https://doi.org/10.3390/en11010216.
[26] J.A. Libra, K.S. Ro, C. Kammann, Y. Funke, A. Berge, N.D. Neubauer, M. Titirici, C. Fühner, O. Bens, J. Kern, K. Emmerich, Hydrothermal carbonization of biomass residuals: a comparative review of the chemistry, processes and applications of wet and dry pyrolysis, Biofuels. 2 (2011) 71–106.
[27] N. Khan, S. Mohan, P. Dinesha, Regimes of hydrochar yield from hydrothermal degradation of various lignocellulosic biomass: A review, J. Clean. Prod. 288 (2021), 125629, https://doi.org/10.1016/j.jclepro.2020.125629.
[28] I. Pavlovič, Ž. Knez, M. Škerget, Hydrothermal reactions of agricultural and food processing wastes in sub- and supercritical water: A review of fundamentals, mechanisms, and state of research, J. Agric. Food Chem. 61 (2013) 8003–8025, https://doi.org/10.1021/jf401008a.
[29] A. Partridge, E. Sermyagina, E. Vakkilainen, Impact of pretreatment on hydrothermally carbonized spruce, Energies. 13 (2020), https://doi.org/10.3390/en13112984.
[30] L. Zhang, S. Liu, B. Wang, Q. Wang, G. Yang, J. Chen, Effect of residence time on hydrothermal carbonization of corn cob residual, BioResources. 10 (2015) 3979–3986, https://doi.org/10.15376/biores.10.3.3979-3986.
[31] E. Sermyagina, J. Saari, J. Kaikko, E. Vakkilainen, Hydrothermal carbonization of coniferous biomass: Effect of process parameters on mass and energy yields, J. Anal. Appl. Pyrolysis. 113 (2015) 551–556, https://doi.org/10.1016/j.jaap.2015.03.012.
[32] L. Yan, Y. Wang, J. Li, Y. Zhang, L. Ma, F. Fu, B. Chen, H. Liu, Hydrothermal liquefaction of Ulva prolifera macroalgae and the influence of base catalysts on products, Bioresour. Technol. 292 (2019), 121286, https://doi.org/10.1016/j.biortech.2019.03.125.
[33] K.P.R. Dandamudi, K. Muhammed Luboowa, M. Laideson, T. Murdock, M. Seger, J. McGowen, P.J. Lammers, S. Deng, Hydrothermal liquefaction of Cyanidioschyzon merolae and Salicornia bigelovii Torr.: The interaction effect on product distribution and chemistry, Fuel. 277 (2020), 118146, https://doi.org/10.1016/j.fuel.2020.118146.
[34] R.B. Carpio, Y. Zhang, C.T. Kuo, W.T. Chen, L.C. Schideman, R. de Leon, Effects of reaction temperature and reaction time on the hydrothermal liquefaction of demineralized wastewater algal biomass, Bioresour. Technol. Reports. 14 (2021), 100679, https://doi.org/10.1016/j.biteb.2021.100679.
[35] L.J. Hansen, S. Fendt, H. Spliethoff, Impact of hydrothermal carbonization on combustion properties of residual biomass, Biomass Convers. Biorefinery. 12 (2022) 2541–2552, https://doi.org/10.1007/s13399-020-00777-z.
[36] X. Cui, M. Lu, M.B. Khan, C. Lai, X. Yang, Z. He, G. Chen, B. Yan, Hydrothermal carbonization of different wetland biomass wastes: Phosphorus reclamation and hydrochar production, Waste Manag. 102 (2020) 106–113, https://doi.org/10.1016/j.wasman.2019.10.034.
[37] S. Seyedsadr, R. Al Afif, C. Pfeifer, Hydrothermal carbonization of agricultural residues: A case study of the farm residues -based biogas plants, Carbon Resour, Convers. 1 (2018) 81–85, https://doi.org/10.1016/j.crcon.2018.06.001.
[38] Z. Luo, W. Tao, CFBC and BFBC of low-rank coals, Elsevier Ltd (2017), https://doi.org/10.1016/B978-0-08-100895-9.00007-3.
[39] A. Shrestha, B. Acharya, A.A. Farooque, Study of hydrochar and process water from hydrothermal carbonization of sea lettuce, Renew. Energy. 163 (2021) 589–598, https://doi.org/10.1016/j.renene.2020.08.133.
[40] M. Karimi, M. Shirzad, Biomass/Biochar carbon materials for CO2 capture and sequestration by cyclic adsorption processes : A review and prospects for future directions, J. CO2 Util. 57 (2022), 101890, https://doi.org/10.1016/j.jcou.2022.101890.
[41] L. Azaare, M.K. Commeh, A.M. Smith, F. Kemausuor, Co-hydrothermal carbonization of pineapple and watermelon peels: Effects of process parameters on hydrochar yield and energy content, Bioresour. Technol. Reports. 15 (2021), 100720, https://doi.org/10.1016/j.biteb.2021.100720.
[42] S.M. Heilmann, H.T. Davis, L.R. Jader, P.A. Lefebvre, M.J. Sadowsky, F. J. Schendel, M.G. von Keitz, K.J. Valentas, Hydrothermal carbonization of microalgae, Biomass and Bioenergy. 34 (2010) 875–882, https://doi.org/10.1016/j.biombioe.2010.01.032.
[43] L. Axelsson, M. Franzén, M. Ostwald, G. Berndes, G. Lakshmi, N.H. Ravindranath, Perspective: Jatropha cultivation in southern India: Assessing farmers' experiences, Biofuels, Bioprod. Biorefining. 6 (2012) 246–256, https://doi.org/10.1002/bbb.
[44] O. Farobie, A. Amrullah, A. Bayu, N. Syaftika, L.A. Anis, E. Hartulistiyoso, In-depth study of bio-oil and biochar production from macroalgae Sargassum sp. via slow pyrolysis, RSC Adv. 12 (2022) 9567–9578, https://doi.org/10.1039/d2ra00702a.
[45] Q. Xu, Q. Qian, A. Quek, N. Ai, G. Zeng, J. Wang, Hydrothermal carbonization of macroalgae and the effects of experimental parameters on the properties of hydrochars, ACS Sustain. Chem. Eng. 1 (2013) 1092–1101, https://doi.org/10.1021/sc400118f.
[46] M. Sevilla, J.A. Maciá-Agulló, A.B. Fuertes, Hydrothermal carbonization of biomass as a route for the sequestration of CO2: Chemical and structural properties of the carbonized products, Biomass and Bioenergy. 35 (2011) 3152–3159, https://doi.org/10.1016/j.biombioe.2011.04.032.
[47] J. Mumme, L. Eckervogt, J. Pielert, M. Diakité, F. Rupp, J. Kern, Hydrothermal carbonization of anaerobically digested maize silage, Bioresour. Technol. 102 (2011) 9255–9260, https://doi.org/10.1016/j.biortech.2011.06.099.
[48] H. Liu, Y. Chen, H. Yang, F.G. Gentili, U. Söderlind, X. Wang, W. Zhang, H. Chen, Hydrothermal carbonization of natural microalgae containing a high ash content, Fuel. 249 (2019) 441–448, https://doi.org/10.1016/j.fuel.2019.03.004.
[49] A. Amrullah, O. Farobie, A. Bayu, N. Syaftika, E. Hartulistiyoso, N.R. Moheimani, S. Karnjanakom, Y. Matsumura, Slow Pyrolysis of Ulva lactuca (Chlorophyta) for Sustainable Production of Bio-Oil and Biochar, Sustain. 14 (2022) 1–14, https://doi.org/10.3390/su14063233.
[50] M. Sevilla, A.B. Fuertes, The production of carbon materials by hydrothermal carbonization of cellulose, Carbon N. Y. 47 (2009) 2281–2289, https://doi.org/10.1016/j.carbon.2009.04.026.
[51] M.M. Titirici, A. Thomas, S.H. Yu, J.O. Müller, M. Antonietti, A direct synthesis of mesoporous carbons with bicontinuous pore morphology from crude plant material

by hydrothermal carbonization, Chem. Mater. 19 (2007) 4205–4212, https://doi.org/10.1021/cm0707408.
[52] A.B.D. Nandiyanto, R. Oktiani, R. Ragadhita, How to Read and Interpret FTIR Spectroscope of Organic Material, Indones, J. Sci. Technol. 4 (2019) 97–118.
[53] A. Iaccarino, R. Gautam, S.M. Sarathy, Bio-oil and biochar production from halophyte biomass: effects of pre-treatment and temperature on Salicornia bigelovii pyrolysis, Sustain, Energy Fuels. 5 (2021) 2234–2248, https://doi.org/10.1039/d0se01664k.
[54] T. Järvinen, D. Agar, Experimentally determined storage and handling properties of fuel pellets made from torrefied whole-tree pine chips, logging residues and beech stem wood, Fuel. 129 (2014) 330–339, https://doi.org/10.1016/j.fuel.2014.03.057.
[55] M.J. Ko, H.H. Nam, M.S. Chung, Subcritical water extraction of bioactive compounds from Orostachys japonicus A. Berger (Crassulaceae), Sci. Rep. 10 (2020) 1–10, https://doi.org/10.1038/s41598-020-67508-2.
[56] R.A. Pratiwi, A.B.D. Nandiyanto, How to Read and Interpret UV-VIS Spectrophotometric Results in Determining the Structure of Chemical Compounds, Indones. J. Educ. Res. Technol. 2 (2022) 1–20, https://doi.org/10.17509/ijert.v2i1.35171.